Jurnal Presipitasi
Media Komunikasi dan Pengembangan Teknik Lingkungan
e-ISSN: 2550-0023

Vol 23, No 2, 2026, 351-373
Article available at homepage presipitasi

Regional Case Study

Flood Risk and Economic Loss Assessment in the Lower Citarum Basin Using InaSAFE

Rahmah Dara Lufira[1*], Suwanto Marsudi[1], Ussy Andawayanti[1], Ery Suhartanto[1], M. Amar Sajali[1], Rizki Ramadhani Pratama[2]

[1] Department of Water Resources Engineering, Universitas Brawijaya, Jalan MT. Haryono 167, Ketawanggede, Lowokwaru, Malang, Jawa Timur, Indonesia 65145

[2] Department of Civil and Environmental Engineering, Nagoya University, Furo-cho, Chikusa-ku, Nagoya, Jepang 464-8603

* Corresponding Author, email: rahmahdara@ub.ac.id

Abstract

The hydrometeorological hazard of flooding in the Lower Citarum River Basin constantly affects agricultural sustainability, infrastructure, settlements, and regional economic activities. This study used InaSAFE to model human exposure and economic losses due to flooding under a 50-year return-period scenario. Flood depths were classified as >1.5 m (high), 0.76–1.5 m (medium), and ≤0.76 m (low) and then overlaid with spatial layers of population, land cover, roads, and buildings. The results revealed 1,739,195 exposed individuals, with 1,067,442 requiring evacuation support from medium-to high-depth classes. The different types of land cover exposed to floods cover 126,413 ha, mainly agricultural areas. The minimum humanitarian relief needs are US$ 88.00 million. The losses from buildings and public facilities totaled USD 616.51 million, and for road infrastructure, they amounted to USD 1.23 million, providing a subtotal of primary direct losses of USD 894.67 million. Additional proxy-based elements raised the stretched notional economic-loss estimate to USD 2.64 billion. These results offer a baseline for additional studies on flood-risk reduction and future scenario-based analyses of possible mitigation alternatives; they are not an explicit evaluation of the hydraulic or economic effectiveness of the Cijurey Dam.

Keywords: Damage valuation; economic loss; flood exposure; InaSAFE; Lower Citarum Basin; mitigation planning

1. Introduction

Flooding is one of the most harmful hydrometeorological hazards worldwide, particularly because rapid construction and land-use change combined with climate variability continue to exacerbate damage (Fox et al., 2024; Sun et al., 2022). Recent syntheses show that urban flood risk is not just a product of hazard intensity, but arises from the triadic interaction among hazard, exposure, and vulnerability, all mediated by data availability, model uncertainty, and governance capacity (Pakati et al., 2025; Pavesi et al., 2024; Ruidas et al., 2024). In Asia, the economic impacts of weather- and water-related extremes have sharply increased in recent decades, emphasizing the need for more impact-based risk information to inform planning, preparedness, and investment prioritization (Alfieri et al., 2024).

Flood events are prevalent in Indonesia, particularly in many of its large river basins, such as those located in West Java, where flooding commonly interrupts settlements via transport systems and agricultural production. National disaster statistics show that hydrometeorological hazards, including floods as one of the major types, account for many of the reported disasters and losses incurred, which require more informed spatially explicit risk analysis of vulnerability and resilience. The importance of catchment factors, such as the expansion of built-up areas, rainfall patterns, topography, and hydrological responses, makes it impossible to disentangle flood occurrence and severity downstream from land and water management upstream in West Java (Kayitesi et al., 2022; Rahayu et al., 2023).

The downstream Citarum River Basin is considered to have strategic socioeconomic importance because of the presence of very dense settlements, industrial activities, and productive agricultural lands. However, its floodplain location and growing vulnerability have led to large expected losses from future major flooding events. The policy question in the Lower Citarum context is not simply to map flood-prone locations but rather to transform flood depth scenarios into actionable information on the affected population, exposed agricultural land, disrupted transport networks, and damaged buildings. This is particularly necessary because the Bekasi-Karawang corridor represents an area of extreme population density, industrial concentration, and floodplain agriculture, all in a common downstream risk zone. For policy and infrastructure planning, including the evaluation of flood-control options such as reservoirs, dams, and complementary non-structural measures, decision-makers require credible estimates of who and what are at risk and how large the potential direct economic losses may be under design-relevant events such as a 50-year return period flood (T = 50 years) (Chitrakar et al., 2023; Pavesi et al., 2024; Ruidas et al., 2024).

Flood impact assessment is generally based on three main components: (i) a hazard layer accounting for flood extent and/or depth, (ii) exposure layers representing population, assets, land use, and infrastructure, and (iii) vulnerability or damage functions transforming hazard intensity into economic losses. Recent studies have shown that results can be sensitive to the assumptions made on vulnerability, such as the definition of points of damage initiation in depth-damage relationships and the treatment of uncertainty and spatial correlation in aggregated loss estimation (Pita et al., 2021; Rahim et al., 2024; Storrøsten et al., 2024). In parallel, practical planning in data-scarce contexts routinely draws on open and semi-open geospatial datasets (e.g., building footprints) and accessible analytical tools, with utility affected by completeness, consistency, and transferability across space (Cerri et al. 2021; Meresa et al. 2021).

Although hazard maps and geospatial exposure datasets are increasingly available, a persistent gap exists in many data-scarce basins: the translation of flood scenarios to impact metrics that are transparent, reproducible, and directly useful for preparedness, mitigation screening, and investment prioritization across sectors. This gap is more context-specific for the Lower Citarum Basin. While current flood-risk information has helped to better understand the drivers of floods, flooded areas, and broad processes operating at a regional scale, less attention has been paid to an operational and reproducible workflow that links a design-relevant depth of flooding with spatially explicit exposure layers and economic valuation employing sector-specific methods. In this regard, we still lack a baseline assessment providing simultaneous estimates of the exposed and affected populations, minimum humanitarian needs, agricultural productivity losses, road disruption, and building-related damages under a common hazard classification.

This gap is particularly relevant in areas where exposure inventories and vulnerability information are incomplete or heterogeneous. In such cases, uncertainty in the representation of hazards and the assumptions of damage functions may propagate, leading to highly variable loss estimates (Cerri et al., 2021; Eilander et al., 2023; Pavesi et al., 2024). Consequently, the literature calls for operational workflows that translate hazard intensity into impact-based risk information that relates inundation characteristics with population consequences and direct economic losses in outputs that are interpretable for practitioners and comparable across scenarios, thereby strengthening evidence-informed planning and flood risk governance (Alfieri et al., 2024; El-Saoud & Othman, 2022; Pakati et al., 2025; Ruidas et al., 2024).

This study applied the InaSAFE impact assessment framework to estimate the potential impacts of a 50-year return period flood (T = 50 years) in the Lower Citarum Basin by integrating flood hazard information with exposure datasets for population, land use, buildings, and roads. The contribution of this study lies in operationalizing InaSAFE as a transparent, multi-sector impact-assessment workflow for the Lower Citarum Basin, rather than developing a new hydrological or hydraulic flood model. By combining an adopted flood depth scenario with harmonized exposure layers and valuation assumptions, this study provides a pre-mitigation baseline that can be compared with future structural and non-structural mitigation scenarios. Specifically, the objectives are to: (1) quantify the exposed and affected population and estimate the minimum humanitarian needs; (2) estimate direct losses associated with agricultural land productivity, road infrastructure, and buildings; and (3) provide an evidence base to support flood-risk management and investment planning in West Java. The results are intended to function as a pre-mitigation baseline for evaluating future mitigation portfolios, including structural interventions and complementary, non-structural measures. This study does not directly evaluate the performance of the proposed Cijurey Dam; rather, it provides downstream exposure and loss estimates to support subsequent scenario-based assessments that would require explicit with- and without-dam modelling, flood-routing analysis, inundation-reduction assessment, and economic feasibility evaluation.

2. Methods

2.1 Study Area

This study was conducted in the Citarum River system, West Java, Indonesia, focusing on (i) the Lower Citarum (Citarum Hilir) floodplain as the primary impact zone and (ii) the Cijurey-Cihoe sub-basin as the upstream structural-mitigation context for the proposed Cijurey Dam. The inclusion of the Cijurey-Cihoe sub-basin was only for planning context purposes; this study did not simulate dam operation, storage effect, flood-peak attenuation, or downstream inundation reduction effects of the planned dam. This framing is appropriate considering that contemporary patterns of downstream flood losses are a strong function of upstream hydrologic response, land cover dynamics, and river-floodplain connectivity in rapidly changing peri-urban landscapes in Java (Kayitesi et al., 2022; Rahayu et al., 2023). In the case of the downstream component, we focused on land-use types in flood-prone areas over the Bekasi-Karawang collapse-induced industrial and settlement corridor, where high population densities and built assets combine to create prospective direct losses during major inundation events. Owing to the heterogeneity and spatially explicit nature of most impact estimations based on exposure, proper prioritization of risk reduction or contingency planning in economic zones that are important but highly exposed is crucial (Pakati et al., 2025; Pavesi et al., 2024).

In the upstream component, this study identifies and maps the Cijurey River as part of the Sukamakmur District area, Bogor Regency, where the tributary network of this river belongs to the Cihoe River in a wider system or network, namely, the Citarum basin system. The planned dam location is at the Cihoe River (area of study), a few meters from the Comas-Cijurey confluence. The land cover composition of the Cihoe Basin, characterized by shrubs, rice fields, dry fields, and plantations, affects runoff generation and sediment dynamics, which are important processes related to downstream flooding (Huang et al., 2022; Kayitesi et al., 2022). The baseline demographic characteristics of the Sukamakmur District, described as village-level population and density, are summarized in Table 1. The baseline agricultural conditions in the Sukamakmur District, including the planted area, harvested area, and rice production, are shown in Table 2.

Table 1. Population, village area, and population density in Sukamakmur District in 2018

No.	Village	Population (people)	Area (km²)	Population density (people/km²)
1.	Sukawangi	9,684	18	538
2.	Sukaharja	6,388	37	173
3.	Wargajaya	7,954	5	1,473
4.	Sirnajaya	7,532	16	480
5.	Sukamulya	8,016	15	531
6.	Sukamakmur	7,466	12	598
7.	Cibadak	8,848	7	1,181
8.	Pabuaran	12,193	18	689
9.	Sukadamai	5,384	16	333
10.	Sukaresmi	6,014	9	652
Subdistrict		79,479	154	515

Table 2. Planted area, harvested area, and rice production in Sukamakmur District in 2018

No.	Village	Planted area (ha)	Harvested area (ha)	Production (tons)
1.	Sukawangi	20.8	20.9	4.3
2.	Sukaharja	22.0	20.4	4.5
3.	Wargajaya	20.2	20.4	4.1
4.	Sirnajaya	20.3	20.9	4.2
5.	Sukamulya	20.3	20.9	4.2
6.	Sukamakmur	18.6	20.5	3.8
7.	Cibadak	19.9	20.9	4.2
8.	Pabuaran	18.6	20.9	3.9
9.	Sukadamai	20.8	20.9	4.3
10.	Sukaresmi	19.5	20.4	4.0
Subdistrict		201.0	207.1	41.5

2.2 Data Collection and Preprocessing

Flood hazard information was compiled from the 2015 Report on the Impact of Natural Disasters on the Bekasi-Karawang Industrial Area, which provides flood inundation mapping for the Citarum Hilir Region. The present study did not generate a new hydrological or hydraulic simulation; instead, it adopted the existing T = 50-year inundation depth scenario from a previously modelled flood-inundation assessment as the baseline hazard input for InaSAFE-based impact and loss estimation. In the source assessment, Lower Citarum flood-inundation maps were generated using Nays2D Flow, with flood inflows introduced through six outlet points representing contributing sub-basins from the Upper Citarum system. The source assessment produced inundation scenarios for 50-, 100-, and 200-year return periods, and the T = 50-year scenario was selected in this study as the design-relevant baseline for the downstream flood-impact assessment. The use of previously modelled inundation scenarios as a hazard baseline is widely adopted to strengthen the spatial realism of flood scenarios and improve risk communication, particularly in areas where dense gauge records or fully calibrated hydrodynamic models are not available (Pavesi et al., 2024; Thao et al., 2020; Zarekarizi et al., 2021). Accordingly, the hazard layer used in this study should be interpreted as an adopted hydrodynamic inundation scenario rather than a newly developed flood model.

The preprocessing of the hazard layer followed standard GIS harmonization steps to ensure compatibility with impact modelling: (i) georeferencing and digitization, where required; (ii) conversion into an InaSAFE-compatible hazard format with a consistent attribute schema; and (iii) alignment of projection, resolution, and spatial extent with the exposure datasets. The adopted inundation depth layer was classified into three hazard classes following the thresholds used in the source assessment and BNPB-based flood hazard classification: low hazard for inundation depth ≤ 0.76 m, medium hazard for 0.76–1.50 m, and high hazard for > 1.50 m. In this study, all population, land cover, road, and building assets located within the inundation footprint were defined as exposed, whereas assets located within the medium and high hazard classes were defined as affected because these depth classes represent flood conditions that generally require evacuation support and are more likely to cause substantial physical damage or functional disruption. This workflow is consistent with recent studies that combine flood depth representation and geospatial analysis to generate decision-support flood information (Nguyen et al., 2023). Such harmonization is critical because mismatches in coordinate reference systems, grid resolution, or study-boundary clipping can propagate biased overlay results and inflate uncertainty in aggregated loss estimates (Pakati et al., 2025; Pavesi et al., 2024).

Exposure data were assembled from institutional reports, official statistical sources, and available geospatial datasets, including population distribution, land use/land cover, agricultural areas, road networks, and building footprint. More specifically, the population exposure layer was derived from WorldPop data for Indonesia in 2020; the land use/land cover layer was obtained from the Indonesian geospatial data portal using the 2017 land cover dataset; agricultural productivity and value parameters were supported by official statistical data; road network and building footprint layers were compiled from available spatial datasets, including OpenStreetMap and institutional sources; and administrative boundaries were used as aggregation units for summarizing InaSAFE impact outputs. Where building footprints or comparable open datasets are used, data completeness and attribute consistency can vary spatially; therefore, cleaning procedures, including topology checks, removal of duplicates, and attribute harmonization by building or asset class, are essential to reduce exposure-related uncertainty in flood loss estimation (Cerri et al., 2021; Pavesi et al., 2024; Riedel et al., 2024). Because the hazard layer and several exposure layers were adopted from secondary spatial datasets, the resulting loss estimates were conditional on the quality, spatial resolution, temporal consistency, and attribute completeness of the source data. This limitation was considered when interpreting the results and is further addressed in the discussion of the uncertainty and policy use of the estimated losses.

All spatial datasets were harmonized in a common projected coordinate system appropriate for metric spatial analysis in West Java before overlay, area, and length calculations were conducted. The adopted flood hazard layer was treated as a depth-class spatial layer derived from the source hydrodynamic inundation mapping; therefore, its effective spatial detail was governed by the resolution, digitization quality, and spatial representation of the source inundation map rather than by a newly generated computational grid. Population data were processed as gridded exposure data, and land cover, road networks, buildings, and administrative boundaries were processed as vector layers. All exposure layers were clipped to the study boundary, checked for spatial consistency, and aggregated by administrative unit and hazard class for subsequent impact and loss estimations.

2.3 Impact Assessment in InaSAFE

Flood impacts were estimated using the InaSAFE plugin within a GIS environment. In this workflow, a hazard layer is overlaid with an exposure layer to generate an impact layer, accompanied by summary statistics for user-defined aggregation units. This overlay-based, scenario-driven approach is consistent with contemporary flood-risk practices that integrate hazards and exposure to produce decision-relevant outputs for emergency management and investment planning (Pakati et al., 2025; Ruidas et al., 2024). InaSAFE analyses were performed using exposure-specific flood impact functions. The flood-depth layer was overlaid with the population layer to estimate the exposed, affected, and evacuation-needing populations; with the land-cover layer to estimate exposed and affected agricultural and non-agricultural areas; with the road-network layer to estimate exposed and affected road lengths; and with the building layer to estimate exposed and affected building counts by category. The outputs were summarized using the administrative aggregation layer, particularly for Bekasi Regency, Karawang

Regency, and Cikarang City, and were further disaggregated by flood depth class. This procedure ensured that each sectoral impact output retained a consistent relationship among hazard intensity, exposed elements, administrative location, and the subsequent economic valuation. Population impacts were computed as both the exposed population, representing all hazard classes within the inundation footprint, and the affected or evacuation-needing population, operationalized in this study as those located in the medium- and high-threat-index classes. A threshold-based classification of the affected population is a common assumption for operational risk assessments to be interpretable and can easily be implemented in humanitarian logistics and evacuation planning processes, although these results still depend on the definition of threat classes and thresholds (Pavesi et al., 2024; Rahim et al., 2024).

The same overlay logic was applied to generate asset and land-use impacts: (i) roads were reported in km as exposed and affected length; (ii) buildings were reported in units as exposed and affected counts; and (iii) agricultural land was quantified in ha by class, including rice fields and plantations. These exposure categories were chosen based on observations that direct flood losses tend to be largely driven by building and infrastructure damage occurring in higher-density urbanization corridors but can include a substantial agricultural component where the value at risk is concentrated in production zones within red- or green-level floodplain areas (Storrøsten et al., 2024; Venkatappa et al., 2021).

2.4 Economic Valuation Assumptions

Using the basic price assumptions framework of the study, economic valuation converted impact outputs such as those on the affected population and area of impacted land and road-surface valuation area based on affected road length, and the number of affected buildings or areas under asset category translated into estimates for direct monetary loss. To improve methodological transparency, the valuation framework was organized into a two-tiered structure: (i) primary direct losses, which can be explicitly traced to InaSAFE-produced affected exposure quantities and unit-cost or unit-value assumptions, and (ii) supplementary proximate loss components based on economic indicators used to signal more indirect potential economic effects under the feasibility-assumption scenario. This is a common practice in flood-risk modelling, where the reliability of loss estimates depends on unit-cost assumptions that are transparent and on how vulnerability (or damage initiation) is represented per exposure category (Pita et al., 2021; Rahim et al., 2024). The unit prices and valuation parameters applied in this study were adopted from the Cijurey Dam economic feasibility valuation framework and related disaster damage assessment assumptions. All monetary estimates are reported in USD, following the valuation tables used in the source assessment. Therefore, the resulting values should be interpreted as scenario-based estimates conditional on the adopted hazard layer, exposure data, depth classification, and unit price assumptions, rather than as observed post-event loss records.

The valuation approach did not calibrate new continuous depth-damage functions based on observed post-event losses. Instead, it applied the source feasibility study valuation logic, in which affected exposure quantities were combined with unit-cost or unit-value assumptions according to exposure type and hazard class. Humanitarian needs were valued using minimum-needs unit prices, agricultural losses were valued using production- and value-based parameters, road losses were estimated from road-surface valuation areas and road-class unit costs, and building losses were estimated using building-category unit values. All monetary values were retained in USD as reported in the source valuation tables; no additional currency conversion, escalation, or re-pricing to a later base year was conducted.

For the basic humanitarian needs, a minimum-needs basket was outlined to cover essential food and water, multiplied by unit prices provided in the economic aspects to obtain the total cost of cross-border assistance. Table 3 presents the minimum-needs items, unit prices, and total costs used in this study. This is aligned with the humanitarian logistics literature, which demonstrates that scenario-based needs and cost quantification to support pre-positioning and resource allocation decisions is warranted, especially when large affected populations can saturate response capacity (Che et al., 2024; Ruidas et al., 2024).

To determine the economic damage in monetary value, the affected areas of rice fields and plantations located between land use classes (rice) and the flood hazard footprint were intersected with the floods, and production and value parameters similar to those in the source dataset were used. The impacts of flooding on croplands are often monetized as the yield of soil in crop production or as proxy estimates in the absence of plot-level loss observations. Regional studies have shown that floods can cause large shocks to agricultural production across Southeast Asian cropland systems (Pavesi et al., 2024; Venkatappa et al., 2021). The lengths and numbers of affected roads and buildings were then multiplied by the unit repair or replacement costs specific to the asset class. Aggregated infrastructure damage may depend on the spatial correlation of damage and the choice of adopted damage thresholds (Papilloud & Keiler, 2021; Storrøsten et al., 2024).

These include minimum humanitarian needs, agricultural productivity losses, road infrastructure losses, and building-related losses (the other direct-loss subtotal within this study). These components are arguably the most directly measurable dollar values because they are derived from the affected quantities of exposure and associated unit-cost or unit-value assumptions. In contrast, indirect commercial losses, non-market tangible losses, and future land-development opportunity components were considered adjunct proxy-based estimates. The percentage multipliers used for these components follow the economic feasibility framework adopted in the source assessment, where broader economic disruption is approximated as a fixed proportion of direct physical losses when empirical post-event loss observations are unavailable.

Because these supplementary components are not independently observed losses and may partly overlap with direct or sectoral economic consequences, they were not interpreted as being equally robust as the primary direct-loss subtotal. To avoid overstating the amount of loss for any given event and prevent potential double counting, the revised analysis separates a direct exposure-based estimate of an involved hazard into a bidirectional indicative economic-loss assessment. Accordingly, the direct-loss subtotal was reported as the primary InaSAFE-based outcome, whereas the total loss, which includes indirect commercial losses, non-market tangible losses, and future land-use opportunity elements, was only shown as a rough planning envelope under this feasibility study's assumptions.

Table 3. Total cost of minimum humanitarian needs

No	Minimum required items	Amount needed	Unit price (USD)	Cost of needs (USD)
1	Relief goods provided weekly			
	Rice	2,994,438	0.87	2,617,585
	Drinking water	18,715,248	0.25	4,612,659
	Clean water	71,652,687	0.02	1,750,982
	Household equipment	213,891	164	35,119,783
2	Help items provided once			
	Toilet	53,475	821	43,901,651
Total cost of minimum requirements				88,002,660

2.5 Validation, Uncertainty, and Sensitivity Treatment

Because this study used an adopted flood-inundation scenario and secondary exposure datasets, the validation procedure focused on internal consistency checks and transparent uncertainty interpretations. Internal checks were performed to ensure that the exposed and affected totals generated by InaSAFE were consistent with the hazard-class definitions used throughout the manuscript. The exposed values were evaluated against the full inundation footprint, whereas the affected values were evaluated against the medium- and high-hazard classes. Sectoral summaries for population, land cover, roads, and buildings were also checked against the corresponding aggregation units before being converted into monetary values.

External validation against observed flood events and post-disaster loss records was limited by data availability. Spatially explicit and sector-disaggregated records of flood depth, asset damage, insurance claims, field verification, and BNPB/BPBD loss data for the same T = 50-year scenario were not available at a resolution compatible with InaSAFE outputs. Therefore, the results should not be interpreted as a reconstruction of a historical flood event or independently validated post-event damage accounting. Instead, they represent a scenario-based impact and economic loss assessment conditional on the adopted hazard layer, exposure inventories, depth-class thresholds, and valuation assumptions. This distinction is important because flood-loss estimates are sensitive to hazard representation, exposure completeness, and damage or valuation assumptions (Cerri et al., 2021; Pavesi et al., 2024; Rahim et al., 2024).

Uncertainty was considered across three main sources: hazard, exposure, and valuation uncertainties. Hazard uncertainty relates to the adopted inundation-depth scenario, including inflow assumptions, hydrodynamic model configuration, topographic representation, and depth classification. Exposure uncertainty arises from the spatial and temporal consistency of population, land cover, roads, and building datasets. Valuation uncertainty arises from the use of unit prices, agricultural production values, building and road damage assumptions, and percentage-based proxy multipliers for supplementary economic components. As a first-order sensitivity screening, a uniform ±10% change in the direct unit-cost assumptions would produce an equivalent ±10% change in the primary direct-loss subtotal, ranging from approximately USD 805.20 million to USD 984.14 million around the reported USD 894.67 million estimate. Although not a substitute for probabilistic uncertainty analysis, this screening provides evidence that the results should be interpreted as estimates that are relevant to planning and contingent on the scenario of interest rather than deterministic loss values. Such methodological choices revealed that uncertainty might also stem from coordinate system harmonization, source map digitization quality, spatial resolution of the adopted hazard layer, overlay operations, and completeness of exposure inventories.

3. Results and Discussion

The impact estimates are read in terms of three dimensions: spatial concentration, reliability of the estimates, and relevance for planning. We assessed spatial concentration by examining how the affected population, land, roads, and buildings were allocated among the hazard classes and aggregation areas. Reliability is addressed by separating exposure-based direct estimates from additional proxy-based economic components and acknowledging uncertainty in hazard, exposure, and valuation assumptions. Policy meaning in terms of evacuation planning, agriculture protection, continuity of infrastructure, and mitigation investment priority.

3.1 Flood Extent and Exposed Population

The T = 50 simulation results in a large flooded area within the Lower Citarum floodplain in Bekasi Regency, Karawang Regency, and Cikarang City (see output hazard and IAansAFE impact). Figure 1 shows the areal coverage of inundation associated with the T = 50-year scenario. The spatial pattern that is observed, consisting of contiguous flood-affected corridors along the entire river-floodplain system, argues for a continued view that connectivity facilitates downstream inundation in heavily anthropogenically altered basins where mid-scale runoff due to rainfall extremes can exceed natural retention (Kayitesi et al., 2022; Rahayu et al., 2023).

The total exposed population, as an aggregate across all hazard classes is over 1.7 million (which includes all types of hazards) InaSAFE estimates the affected/evacuation-needing population (i.e.by definition: medium and high hazard classes) exceed 1 million people (1,067,442). The figures corrected in this manner were consistent within each hazard class total and were used throughout this manuscript. Figure 2 shows the spatial distribution of the affected population, which we have mapped to the Lower Citarum floodplain level. The population distribution exposed by hazard class was as follows: high depth

> 1.5 m (611,146 people), medium depth 0.76–1.5 m (456,296 people), and low depth ≤0.76 m (671,753 people). This class-based characterization is in line with impact-oriented flood risk practices, where depth thresholds increase interpretability for response planning and prioritization of protective measures during an event (Pavesi et al., 2024; Ruidas et al., 2024).

The high proportion of affected people in the mid-high inundation classes indicates that floods are not only expansive but also severe in terms of their displacement potential, with critical consequences for evacuation routes, shelter capacity, and the continuity of vital services. In rapidly developing urban areas, where improvements in protective infrastructure cannot keep pace with the growth in exposure, translating hazard maps into population-impact metrics is important to facilitate actionable risk governance (Pakati et al., 2025; Pavesi et al., 2024).

From a reliability perspective, these population estimates primarily serve to identify relative spatial priorities rather than deterministic evacuation counts. The final exposed population, consisting of 1,067,442 people (61.4% of the total exposed), is consequently mostly represented in depth classes that are operationally relevant for both evacuation and emergency support. This emphasizes the need for policymakers to ensure the continuity of evacuation routes, temporary shelter capacity, and emergency logistics in areas where medium. However, the absolute population totals remain conditional on the adopted flood depth layer, population grid, and depth-class thresholds.

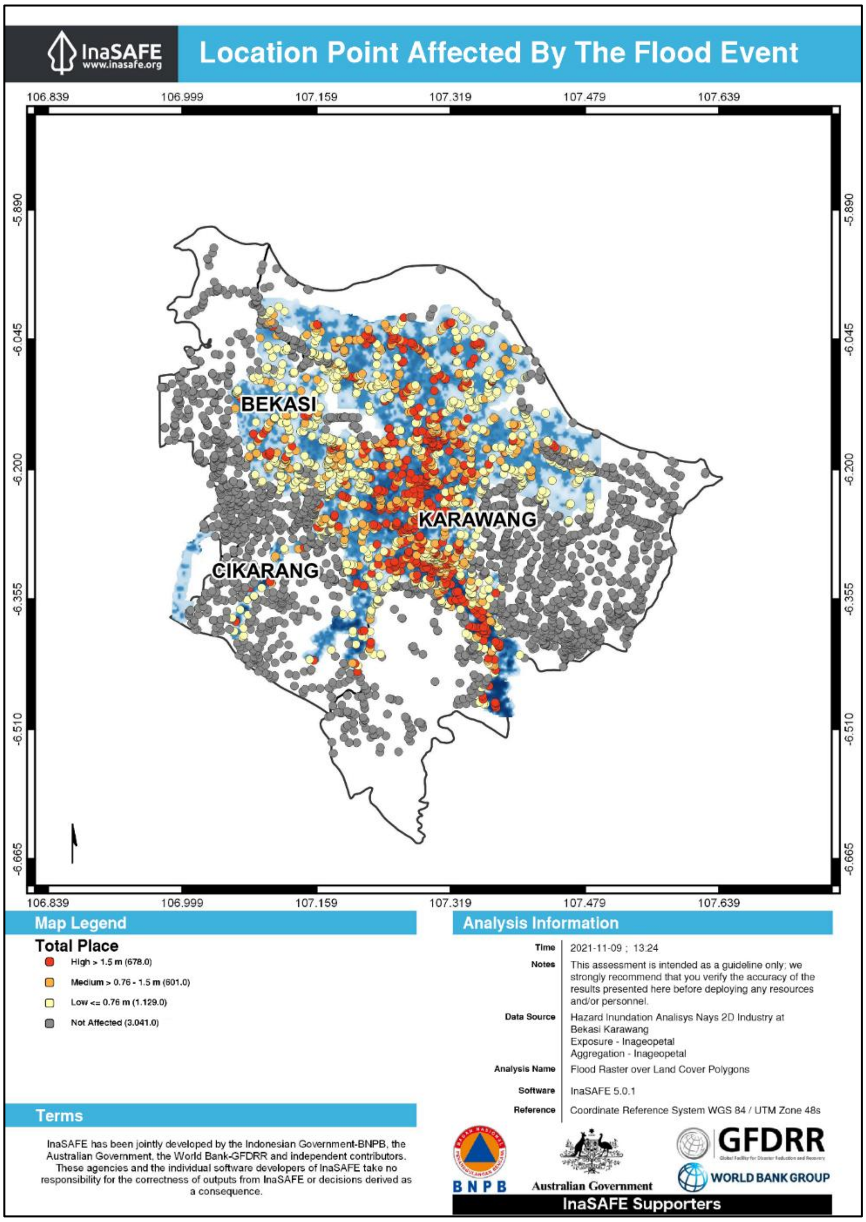

Figure 1. Flood inundation in the Lower Citarum River Basin (T = 50 years)

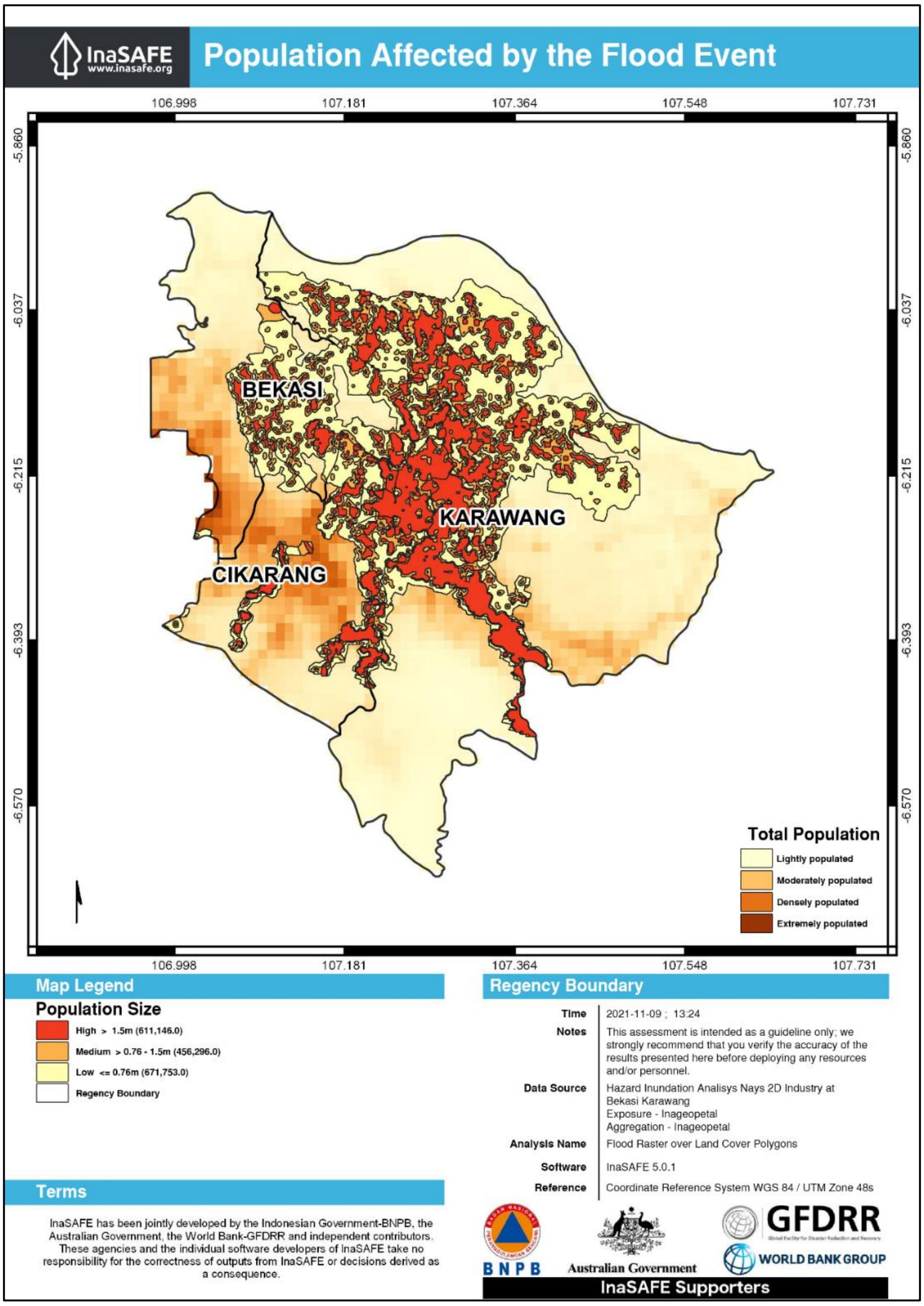

Figure 2. Spatial distribution of population affected by the 50-year flood in the Lower Citarum Basin

3.2 Agricultural Land Productivity Losses

The land-cover impact output indicated a substantial flood footprint across productive landscapes, with a total land-cover exposure of 126,413 ha and an affected land cover of 72,016 ha in the medium- and high-hazard classes. The areas of affected land by land cover class are shown in Figure 3. Depth-class mapping further shows that the affected land cover is concentrated under high depth > 1.5 m (38,421 ha) and medium depth 0.76-1.5 m (33,595 ha), while low depth ≤ 0.76 m (54,397 ha) contributes to broader exposure. This pattern is consistent with evidence that floodplain agricultural systems have heterogeneous flood depths that translate into spatially uneven effects on cropping intensity and yield stability (Kayitesi et al., 2025; Kayitesi et al., 2022; Venkatappa et al., 2021). The assessment showed high vulnerability in agriculture due to rice fields (102,796.79 ha) and plantations (3,744.49 ha). This indicates that the flood scenario matches exactly where food is produced in large volumes throughout the basin.

This is an important consideration because rice systems are particularly sensitive to the duration and depth of flooding, and successive events may interfere with the planting calendar, damage standing crops, or change soil conditions due to erosion or nutrient loss (Kayitesi et al., 2022; Venkatappa et al., 2021).

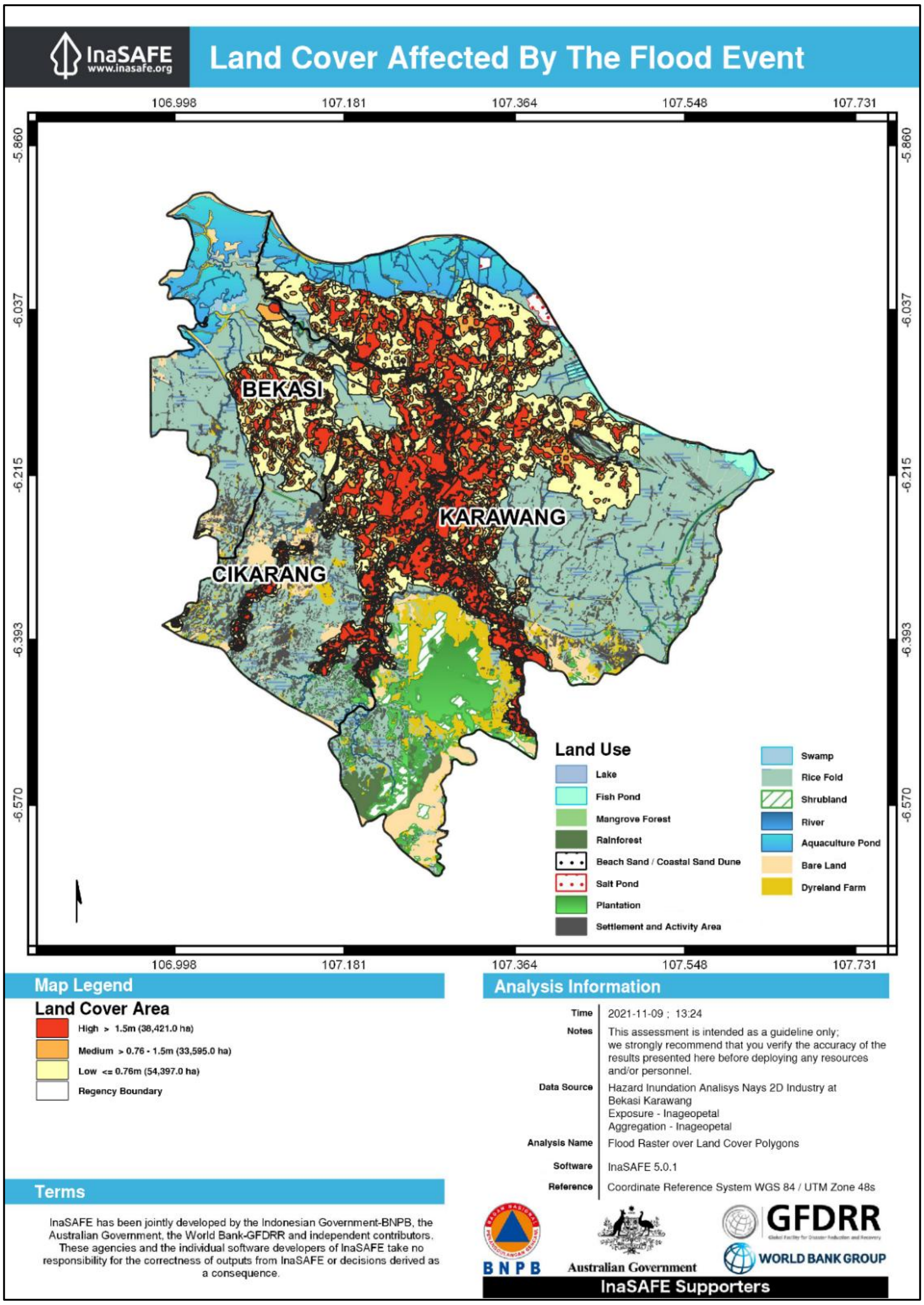

Figure 3. Spatial distribution of land affected by the 50-year flood in the Lower Citarum Basin

Based on the reported production, value parameters, and unit-price assumptions, the estimated agricultural land productivity loss for exposed cropland totals USD 188,931,306, overwhelmingly dominated by rice fields (USD 183,731,509) relative to plantations (USD 5,199,797). The estimated agricultural productivity losses by aggregation unit are reported in Table 4. The dominance of rice-related losses is consistent with regional findings that flood-induced shocks in Southeast Asian croplands are often driven by staple cereal systems with large cultivated extents and high exposure to low-lying plains (Venkatappa et al., 2021; Zhang et al., 2021).

The spatial distribution of agricultural losses has direct policy implications. Karawang accounts for the largest share of agricultural productivity losses, with rice-field and plantation losses totaling approximately USD 112.48 million, or approximately 59.5% of the total agricultural loss. This reflects the concentration of productive floodplain agriculture within the inundation footprint and indicates that flood-risk reduction in the Lower Citarum Basin is also a food production and livelihood protection issue. The reliability of this estimate is strongest as a screening-level indicator of the exposed agricultural value, but it should not be interpreted as a plot-level crop-loss observation because the valuation relies on production- and value-based proxies rather than crop stage, inundation duration, or post-event yield-loss measurements.

Table 4. Total loss of land productivity in each aggregation area

Regency /city	Land type	Land area (ha)	Total production (kw)	Total production cost (USD)	Total production value (USD)
Bekasi	Ricefield	28,628.46	1,493,832.83	37,472,338	51,168,421
	Plantation	760.68	29,164.29	748,805	1,056,315
Karawang	Ricefield	61,454.98	3,206,720.64	80,439,603	109,840,156
	Plantation	1,900.43	72,862.52	1,870,775	2,639,041
Cikarang	Ricefield	12,713.36	663,383.02	16,640,759	22,722,932
City	Plantation	1,083.38	41,536.84	1,066,475	1,504,446
Amount	Ricefield	102,796.79	5,363,936.49	134,552,701	183,731,509
	Plantation	3,744.49	143,563.65	3,686,055	5,199,797
Grand total					188,931,306

3.3 Road Exposure and Functional Disruption

The road-network overlay results indicated that 5,901.804 km of roads were exposed to flooding and 3,429.733 km were affected under the medium and high hazard classes. These values represent the road network length outputs from InaSAFE, not the road surface area used for monetary damage valuation. The distribution of the affected road segments in the flood scenario is shown in Figure 4. The hazard-class distribution shows 1,835.235 km under a high depth of > 1.5 m, 1,594.498 km under a medium depth of 0.76–1.5 m, and 2,472.071 km under a low depth of ≤ 0.76 m, indicating that a large share of the network is not merely exposed but is likely to experience operational failure or severe service degradation. This pattern is in line with the transport-flood literature, which states that the partial loss of critical links can disproportionately impair system performance because of the network topology and the location of critical corridors (Papilloud & Keiler, 2021; Ruidas et al., 2024).

The unit-cost approach estimates the direct loss valuation for the road infrastructure at USD 1,228,389 . However, the valuation table lists road-surface area equivalents in km², not road-network lengths in km. In the source valuation framework, road lengths were transformed into road-surface valuation areas using road-class width assumptions, hazard-class damage factors, and unit-cost values. Thus, the reported road lengths above and the valuation areas in Table 5 are not directly comparable metrics. This clarification accounts for the apparent contradiction between the InaSAFE road length totals and the lower numerical values used in the road damage valuation table.

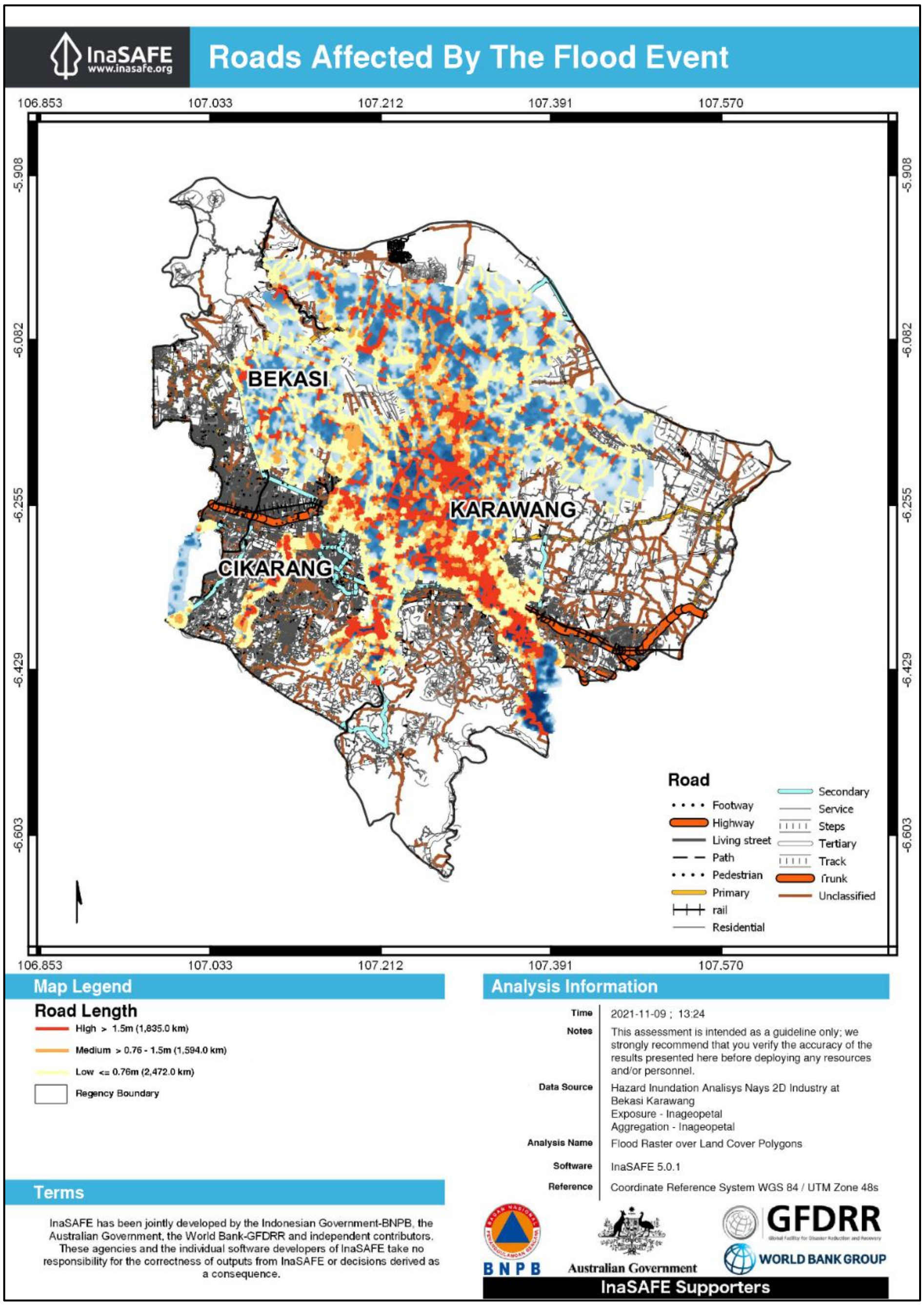

Figure 4. Spatial distribution of roads affected by the 50-year flood in the Lower Citarum Basin

The estimated direct road damage losses by aggregation unit are presented in Table 5. Studies based on accessibility highlight that road flooding leads to cascading effects across service areas, especially when alternative routes are limited and equally exposed (Papilloud & Keiler, 2021; Storrøsten et al., 2024). The heavy concentration of potentially affected road lengths in the medium-to-high hazard classes sustains prioritization from a risk-management viewpoint for (i) protection of critical links, (ii) elevation and drainage improvements at recurrent bottlenecks, and (iii) contingent routing for emergency services. New work highlights the importance of conveying uncertainty in making credible decisions about flood risk for linear infrastructure, considering the spatial correlation among damage drivers that can significantly affect loss estimates at an aggregate level as well as serviceability (Pavesi et al., 2024; Storrøsten et al., 2024).

Our findings on road impacts provide a crucial distinction between monetary loss and functional importance. Despite being low in comparison to total building and agricultural losses, the indirect road-damage cost is significant, given that 3,429.733 km (58.1% of the exposed road length) of the exposed road network lies within the medium-high hazard classes. This suggests that road exposure is probably more relevant for policy for potential disruption to evacuation and/or emergency relief, supply chains, and access to essential services than for replacing the cost of a road. Road-related mitigation should focus on essential links and corridors that are recurrently flooded rather than just post-event repair-cost estimates.

Table 5. Road-surface valuation area and estimated road-damage losses in each aggregation area

Regency/ city	Road class	Hazard class						Total	
		High		Medium		Low			
		Road area (km^2)	Loss cost (USD)	Road area (km^2)	Loss cost (USD)	Road area (km^2)	Loss cost (USD)	Road area (km^2)	Loss cost (USD)
Bekasi	Local	2.397	130,666	2.143	58,400	3.389	18,470	7.929	207,536
	Other	0.054	2,961	0.029	801	0.025	137	0.109	3,899
	Path	0.160	8,741	0.135	3,690	0.228	1,241	0.523	13,671
	Arteries	0.026	2,878	0.032	1,754	0.129	1,408	0.188	6,041
	Collector	0.144	15,680	0.149	8,106	0.264	2,876	0.556	26,663
	Toll	0.187	-	0.021	-	0.007	-	0.214	-
Karawang	Local	7.454	406,269	5.242	142,850	8.381	45,676	21.077	594,794
	Other	0.133	7,255	0.133	3,626	0.163	889	0.429	11,770
	Path	0.187	10,178	0.139	3,797	0.296	1,614	0.622	15,589
	Arteries	0.362	39,473	0.305	16,620	0.246	2,682	0.913	58,775
	Collector	0.266	28,988	0.197	10,733	0.357	3,892	0.820	43,614
	Toll	0.650	-	0.494	-	0.529	-	1.674	-
Cikarang City	Local	2.083	113,548	3.006	81,927	4.532	24,698	9.621	220,173
	Other	0.047	2,556	0.077	2,111	0.095	518	0.219	5,185
	Path	0.073	3,979	0.077	2,093	0.109	593	0.259	6,665
	Arteries	0.035	3,837	0.013	733	0.014	151	0.063	4,722
	Collector	0.038	4,161	0.071	3,884	0.114	1,247	0.224	9,292
	Toll	0.393	-	0.394	-	0.197	-	0.983	-
Total cost-bearing road-surface valuation area								43.553	1,228,389

3.4 Building Exposure and Direct Damages

Exposure analysis of buildings based on the inundation footprint showed that 312,215 buildings were exposed, with 169,771 adversely impacted within the medium-to-high hazard definition. The spatial distributions of the affected buildings are shown in Figure 5. The depth-class breakdown indicates 83,040 buildings with high depth > 1.5 m, 86,731 buildings with medium depth 0.76-1.5 m; and 142,444 buildings with low depth ≤ 0.76 m, showing that building impacts are both common and extreme across the most damaging inundation classes. The depth-stratified exposure pattern is consistent with flood-vulnerability studies that demonstrate non-linear increases in damage severity at greater depths and durations, especially in areas with denser settlements (Pita et al., 2021; Rahim et al., 2024; Tu et al., 2023).

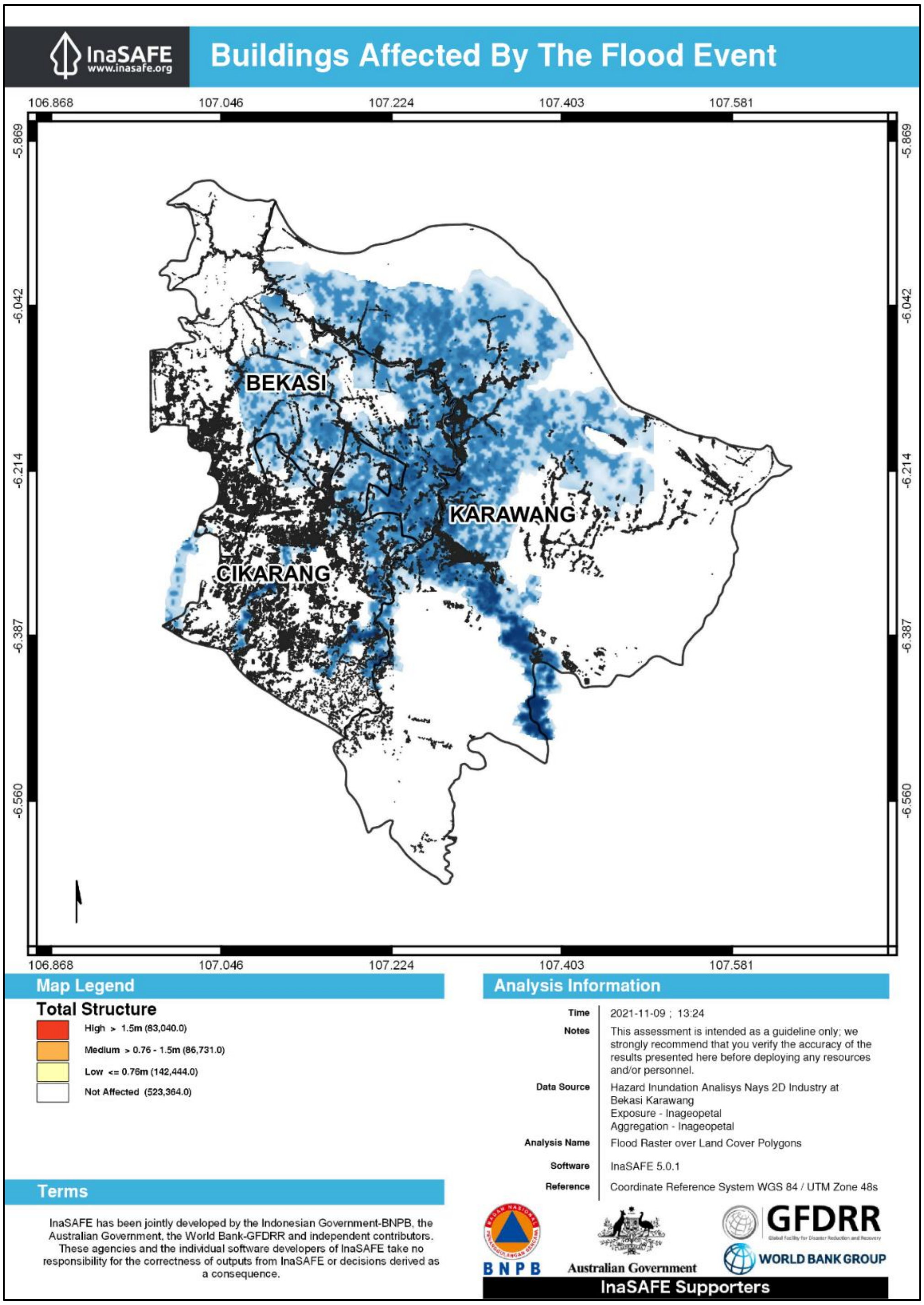

Figure 5. Spatial distribution of buildings affected by the 50-year flood in the Lower Citarum Basin

According to the reported unit prices and asset categories, a direct building-related loss of USD 616,508,593 was incurred, mainly attributable to settlement or residential structures (USD 360093464), public facilities (USD 110177677), education (USD 42934887), and bridges (USD $43.492315). The building-summary losses due to direct damage by category are summarized in Table6. The predominance of losses from residential and public assets is consistent with the empirical evidence observed in many urbanizing basins, where aggregate flood risk can be predicted by an interplay between concentrations of exposure (the exposed structures) and vulnerability (e.g., buildings providing essential services where rapid restoration is crucial after flooding; Pita et al., 2024; Pita et al., 2021).

Table 6. Total value of building damage losses

Building type	Hazard class					
	High		Medium		Low	
	Total (unit)	Loss cost (USD)	Total (unit)	Loss cost (USD)	Total (unit)	Loss cost (USD)
Education	3,597	39,212,854	683	3,722,033	0	-
Government	0	-	2,732	14,888,134	0	-
Places of worship	1,199	13,070,951	4,780	26,054,234	4,732	5,158,427
Settlement (m^2)	1,343,564	193,746,200	847,105	69,803,007	4,686,512	96,544,257
Commercial	1,199	235,264	1,366	133,986	13,724	269,255
Public facilities	4,797	52,283,805	9,561	52,108,468	1,893	2,063,371
Evacuation site	0	-	683	3,722,033	0	-
Total		298,549,074		170,431,895		104,035,309

In estimating direct building losses, the sensitivity of the outcomes to assumptions on vulnerability needs to be considered, including the threshold at which damage starts (e.g., the threshold depth at which damage starts) and the representativeness of exposure inventories, especially when building attributes are generalized or derived from open datasets. Recent studies have shown that small differences in depth-damage parametrization can lead to large differences in loss estimates, highlighting the necessity of transparent assumptions and, where possible, local calibration with post-event observations (Cerri et al., 2021; Rahim et al., 2024).

To integrate the sector-specific estimates reported above, Table 7 consolidates the primary direct-loss components associated with the T = 50-year flood scenario across humanitarian minimum needs, agricultural land productivity, road infrastructure and buildings. The table also reports supplementary proxy-based economic components, including indirect economic losses, non-market tangible losses, and future land-development opportunity components, which were adopted from the feasibility study valuation framework to indicate the broader potential economic magnitude of flooding. Presenting results in a single cross-sector summary strengthens the interpretability for decision-making because it links spatial exposure outputs to comparable monetary metrics and facilitates prioritization across competing risk-reduction needs. Such integrated, impact-based accounting is increasingly recommended to move from hazard description to actionable risk information for planning and resource allocation (Pavesi et al., 2024; Ruidas et al., 2024). However, to avoid overstatements, the direct-loss subtotal and supplementary proxy-based components were interpreted separately in this study.

Table 7. Recapitulation of direct losses and supplementary proxy-based economic loss components under the downstream Citarum flood scenario (T = 50 years)

No.	Component	Total	Unit price (USD)	Loss cost (USD)
I	Minimum humanitarian needs			88,002,660
1	Rice (kg)	2,994,438	0.87	2,617,585
2	Drinking water (l)	18,715,248	0.25	4,612,659
3	Clean water (l)	71,652,687	0.02	1,750,982
4	Household equipment (unit)	213,891	164	35,119,783
5	Toilet (unit)	53,475	821	43,901,651

No.	Component	Total	Unit price (USD)	Loss cost (USD)
II	Agricultural land loss exposed (ha)			188,931,306
1	Rice fields	102,796.79	1,787	183,731,509
2	Plantation	3,744.49	1,389	5,199,797
III	Road infrastructure losses based on road-surface valuation area (km²)			1,228,389
1	Local	38.628	54,502	1,022,504
2	Other	0.758	54,502	20,854
3	Path	1.404	54,502	35,925
4	Arteries	1.163	109,003	69,538
5	Collector	1.600	109,003	79,568
6	Toll	2.871	-	-
IV	Loss of exposed buildings (unit)			616,508,593
1	Education	4,280	10,900	42,934,887
2	Government	2,732	10,900	14,888,134
3	Places of worship	10,712	10,900	44,283,612
4	Settlement (m²)	6,877,182	196	360,093,464
5	Commercial	16,289	196	638,504
6	Public facilities	16,933	10,900	110,177,677
7	Bridge	846	109,003	43,492,315
Reported total direct losses				894,670,947
V	Supplementary indirect economic losses			
1	Settlement	15%	894,670,947	134,200,642
2	Agricultural	10%	894,670,947	89,467,095
3	Commercial	37%	894,670,947	331,028,250
4	Industry	45%	894,670,947	402,601,926
5	Public buildings	34%	894,670,947	304,188,122
6	Highway	25%	894,670,947	223,667,737
7	Railroad	23%	894,670,947	205,774,318
Total supplementary indirect economic losses				1,690,928,090
VI	Non-market tangible losses			
1	Losses of affected working population (20%)	870,598	243	42,355,235
Total non-market tangible losses				42,355,235
VII	Future land development advantages			
1	Land development advantages (5%)	435,299	243	10,588,809
Total future land development profit				10,588,809
Expanded indicative economic-loss estimate				2,638,543,081

Table 7 should be interpreted in a hierarchical manner. Components I–IV represent the primary direct-loss subtotal because they are calculated from the affected exposure quantities and unit-cost or unit-value assumptions. These components include minimum humanitarian needs, agricultural productivity losses, road-infrastructure losses, and building-related losses, resulting in reported direct losses of USD 894,670,947. In contrast, Components V–VII represent supplementary proxy-based economic components adopted from the feasibility study valuation framework. These components are included to indicate broader potential economic consequences, but they are not independently observed losses and may partly overlap with direct or sectoral economic impacts. Therefore, the expanded indicative economic loss estimate of USD 2,638,543,081 should not be interpreted as a deterministic or independently validated estimate of the total flood damage. Instead, it represents a planning-oriented economic envelope under the adopted valuation assumptions, whereas the reported direct loss subtotal remains the most directly traceable result of the InaSAFE-based assessment.

The sectoral breakdown of the subtotal of direct losses provides further insight into policy priorities. Of the reported direct losses, approximately 68.9% are losses related to buildings, 21.1% are losses in agricultural productivity, 9.8% are minimum humanitarian needs, and 0.1% are losses to road infrastructure. For example, this distribution means that the largest component of direct loss would be addressed by reducing the physical vulnerability of residential buildings and public facilities, while reducing agricultural risk and preparedness for evacuation are important complementary priorities. However, the small monetary fraction of road losses should not be interpreted as low policy relevance because road disruption can have cascading effects on evacuation, logistics, and service accessibility that are not fully captured by direct repair cost estimates.

Uncertainty and sensitivity considerations also suggest that the reported monetary values should be interpreted with caution. The direct-loss subtotal is the most traceable estimate, as it is associated with affected exposure quantities and unit cost assumptions; however, it is still sensitive to the adopted flood depth classification, exposure inventories, and valuation parameters. A first-order sensitivity screening of the direct unit cost assumptions at the ±10% level indicates that the primary direct-loss subtotal could range from approximately USD 805.20 million to USD 984.14 million. Conversely, the augmented indicative estimate of economic loss is more uncertain because it contains more proxy-based components based on percentage multipliers rather than on loss data that are observed independently. Therefore, these results provide a basis for planning and prioritization; however, further validation using observed flood extents, post-event damage records, field verification, and locally calibrated vulnerability functions is necessary to yield more robust probabilistic loss estimates.

Table 7 summarizes the loss profiles. Direct economic impacts are primarily driven by the exposure and vulnerability of built environments and critical infrastructure. Agricultural losses and short-term humanitarian needs continue to be important components that require dedicated preparedness and response capacity. This pattern is consistent with scenario-based flood-loss estimates in highly exposed floodplains, where damage totals are driven by asset concentrations and the representation of damage initiation and depth-damage relationships for different asset classes (Pita et al., 2021; Rahim et al., 2024). Thus, the direct-loss subtotal and the expanded indicative economic-loss estimate should be understood as scenario-dependent estimates, the magnitude of which is sensitive to hazard classification thresholds and unit-cost or vulnerability assumptions, and not as deterministic post-event accounting values (Pavesi et al., 2024; Rahim et al., 2024).

Table 7 provides a practical baseline for screening intervention portfolios from the risk management perspective. Reducing the structural vulnerability of buildings and protecting essential facilities can directly reduce the largest direct-loss components. Maintaining road functionality can ensure accessibility for evacuation and relief logistics and reduce cascading service disruptions. Studies on transport risk indicate that the functional consequences of flooding on road networks can be disproportionate and that the aggregated estimates of infrastructure risk are influenced by the spatial correlation and uncertainty in damage drivers (Papilloud & Keiler, 2021; Storrøsten et al., 2024). The baseline in Table 7 can thus be used for future scenario comparisons to evaluate alternative mitigation options and progressively include locally validated indirect losses, such as business interruption, leading to a more comprehensive assessment of flood consequences (Endendijk et al., 2024). The baseline developed in this study should be used as a reference condition for further analyses of structural measures, such as the proposed Cijurey Dam, but not as direct evidence of dam performance. Rigorous dam-planning evaluation requires an explicit comparison of without-dam and with-dam scenarios, including reservoir operation, storage effects, flood-peak reduction, downstream inundation changes, residual risk, and benefit-cost assessment.

3.5 Synthesis of Loss Concentration, Robustness, and Mitigation Priorities

The results show that flood losses in the Lower Citarum Basin are concentrated in areas with medium-to-high inundation depths coupled with dense settlements, productive agricultural lands, and critical infrastructure in the Bekasi–Karawang–Cikarang corridor. Building-related losses dominate the reported direct-loss subtotal (approximately 68.9%), mainly because residential structures and public facilities are more broadly exposed and have relatively high unit repair or replacement values. The second largest component is the loss in agricultural productivity, which accounts for approximately 21.1%, with Karawang contributing the largest share owing to its large exposed rice-field area. Road infrastructure losses are only a small monetary share, but road exposure remains highly policy-relevant because the disruption of critical links can have consequences for evacuation, emergency response, supply chains, and access to essential services (Papilloud & Keiler, 2021; Storrøsten et al., 2024).

The robustness of the estimates varies according to the component. The subtotal of direct loss is the most traceable estimate because it is based on the affected quantities of exposure and the assumptions of unit cost or unit value. Conversely, supplementary proxy-based economic components are less robust because they rely on percentage multipliers rather than independently observed post-event loss data. Therefore, the direct-loss subtotal should be the main basis for prioritization, whereas the expanded indicative economic-loss estimate should be interpreted as a planning economic envelope.

The results indicate several priorities for intervention, such as reducing the vulnerability of buildings in the medium-to high-hazard zone, protecting public facilities that are important for the public, strengthening evacuation routes and shelter capacity, maintaining the functionality of critical road links, and improving flood preparedness in highly exposed rice-producing areas, especially in Karawang. The baseline developed in this study could be useful for future comparisons of structural and nonstructural mitigation scenarios. However, the direct evaluation of dam performance requires explicit with and without dam modelling, downstream inundation comparison, residual risk assessment, and benefit-cost assessment.

4. Conclusions

This study presents an impact-based flood assessment for the Lower Citarum River Basin by combining a 50-year return period flood scenario with spatial exposure data on population, agricultural land, road networks, and buildings using InaSAFE. The results indicate that the flood impacts are widespread and spatially concentrated in the Bekasi-Karawang corridor, where dense settlements, productive agricultural areas, and critical transport infrastructure coincide with the inundation footprint. The exposed population in the assessed scenario was 1,739,195, and 1,067,442 people were in the medium-to-high hazard classes, which indicates a large evacuation demand and short-term assistance needs. Agricultural impacts are also considerable, with widespread flooding of rice fields and plantations resulting in an estimated productivity loss of USD 188.93 million. Road impacts were widespread, with 5,901 km exposed and 3,429 km affected, indicating a high likelihood of disrupted mobility and constrained access during emergency response and early recovery. Building impacts dominated the direct-loss profile, with 312,215 buildings exposed and 169,771 impacted. The estimated direct building loss was USD 616.51 million, dominated by residential structures and public facilities. The main exposure-based monetary estimate produced by the InaSAFE analysis is the direct-loss subtotal reported as USD 894.67 million, which includes minimum humanitarian needs, agricultural productivity losses, road infrastructure losses, and building-related losses. The extended indicative economic loss estimate that includes the supplementary proxy-based components is USD 2.64 billion; however, this must be interpreted as a planning-oriented economic envelope based on the valuation assumptions adopted and not a deterministic or independently validated estimate of observed flood damage. Overall, the results provide a quantitative baseline to support the prioritization of risk reduction measures, strengthen preparedness planning, and evaluate mitigation options, including structural interventions and complementary non-structural strategies. The results should not be interpreted as a direct evaluation of the proposed Cijurey Dam because the study does not include dam operations, reservoir storage effects, flood-peak reduction, downstream inundation reduction, residual risk, or benefit-cost performance. Future work should involve improving hazard representation, improving exposure inventories, validating the estimates against observed flood extents and post-event damage records, and extending the assessment to include uncertainty characterization, locally calibrated vulnerability functions, locally validated indirect economic-loss data, and explicit with and without mitigation scenario modelling to achieve more robust, risk-informed decision-making.

Acknowledgement

The authors would like to thank the organizations that provided the necessary data and technical support, especially the Water Resources Engineering Consultant at PT. Bhawana Prasasta and the Central Bureau of Statistics (BPS) Bogor. We also thank all collaborating partners, researchers, and stakeholders for their valuable contributions to improving the understanding of flood risk, strengthening flood hazard assessment, and supporting the development of management plans that integrate environmental and ecological considerations.

Ethics Statement

This study used secondary, aggregated geospatial, and statistical data from government publications, institutional reports, and spatial exposure datasets. The study did not involve human participants, human interviews, human clinical intervention, animal experiments or the use of personally identifiable information. Thus, formal ethical approval and informed consent were not necessary for this research. All data were used solely for academic purposes and in compliance with applicable institutional standards and data-provider terms.

CRedit Author Statement

Rahmah Dara Lufira: Conceptualization, Methodology, Formal Analysis, Writing - Original Draft, Writing – Review & Editing, and Supervision. **Suwanto Marsudi:** Conceptualization, Methodology, Validation, Writing - Review & Editing, and Supervision. **Ussy Andawayanti:** Formal Analysis, Validation, Visualization, Writing - Review & Editing. **Ery Suhartanto:** Supervision, Writing - Review & Editing, Validation. **M. Amar Sajali:** Investigation, Validation, Supervision. **Rizki Ramadhani Pratama:** Investigation, Data Curation, Validation.

Declaration of Artificial Intelligence Use

The authors used Quillbot and SciSpace during the writing of this manuscript to help with language polishing, discovery of literature and clarification of causal interpretation. These tools were not used for data analysis, making scientific decisions, or generating results. The authors have reviewed, verified and edited all the content and assume full responsibility for the integrity and accuracy of the article.

References

Alfieri, L., A. Libertino, L. Campo, F. Dottori, S. Gabellani, T. Ghizzoni, A. Masoero, L. Rossi, R. Rudari, N. Testa, E. Trasforini, A. Amdihun, J. Ouma, Y. Tramblay, H. Wu, and M. Massabò. 2024. Impact-based flood forecasting in the Greater Horn of Africa. Natural Hazards and Earth System Sciences 24(1), 199-224.

Cerri, M., M. Steinhausen, H. Kreibich, and K. Schröter. 2021. Are OpenStreetMap building data useful for flood vulnerability modelling? Natural Hazards and Earth System Sciences 21(2), 643-662.

Che, A., J. Li, F. Chu, and C. Chu. 2024. Optimizing emergency supply pre-positioning for disaster relief: A two-stage distributionally robust approach. Computers & Operations Research 166, 106607.

Chitrakar, P., A. Sana, and S.H.N. Almalki. 2023. Regional distribution of intensity-duration-frequency relationships in Sultanate of Oman. Journal of King Saud University - Science 35(7), 102804.

Eilander, D., A. Couasnon, F.C. Sperna Weiland, W. Ligtvoet, A. Bouwman, H.C. Winsemius, and P.J. Ward. 2023. Modeling compound flood risk and risk reduction using a globally applicable framework: A pilot in the Sofala province of Mozambique. Natural Hazards and Earth System Sciences 23(6), 2251-2272.

El-Saoud, W.A. and A. Othman. 2022. An integrated hydrological and hydraulic modelling approach for flash flood hazard assessment in eastern Makkah city, Saudi Arabia. Journal of King Saud University - Science 34(4), 102045.

Endendijk, T., W.J.W. Botzen, H. de Moel, K. Slager, M. Kok, and J.C.J.H. Aerts. 2024. Enhancing resilience: Understanding the impact of flood hazard and vulnerability on business interruption and losses. Water Resources and Economics 46, 100244.

Fox, S., F. Agyemang, L. Hawker, and J. Neal. 2024. Integrating social vulnerability into high-resolution global flood risk mapping. Nature Communications 15(1), 3155.

Huang, X., B. Xu, P. Zhong, H. Yao, H. Yue, F. Zhu, Q. Lu, Y. Sun, R. Mo, Z. Li, and W. Liu. 2022. Robust multiobjective reservoir operation and risk decision-making model for real-time flood control coping with forecast uncertainty. Journal of Hydrology 605, 127334.

Kayitesi, N.M., A.C. Guzha, and G. Mariethoz. 2022. Impacts of land use land cover change and climate change on river hydro-morphology: A review of research studies in tropical regions. Journal of Hydrology 615, 128702.

Keya, D.R., H.O. Salih, A.E.P. Hayder, and A.O. Mawlood. 2025. Spatial mapping and assessment of soil erodibility using GIS in the middle of Erbil Province. Iraqi Journal of Agricultural Sciences 56(2), 827-837.

Meresa, H., C. Murphy, R. Fealy, and S. Golian. 2021. Uncertainties and their interaction in flood hazard assessment with climate change. Hydrology and Earth System Sciences 25(9), 5237-5257.

Nguyen, H.D., D.K. Dang, Y.N. Nguyen, C.P. Van, Q.-H. Truong, Q.-T. Bui, and A.-I. Petrisor. 2023. A framework for flood depth using hydrodynamic modeling and machine learning in the coastal province of Vietnam. Vietnam Journal of Earth Sciences 45(4), 456-478.

Pakati, S.S., C. Shoko, and T. Dube. 2025. Integrated flood modelling and risk assessment in urban areas: A review on applications, strengths, limitations and future research directions. Journal of Hydrology: Regional Studies 61, 102583.

Papilloud, T. and M. Keiler. 2021. Vulnerability patterns of road network to extreme floods based on accessibility measures. Transportation Research Part D: Transport and Environment 100, 103045.

Pavesi, L., E. Volpi, and A. Fiori. 2024. Flood risk assessment through large-scale modeling under uncertainty. Natural Hazards and Earth System Sciences 24(12), 4507-4522.

Pita, G.L., B.S. Albornoz, and J.I. Zaracho. 2021. Flood depth-damage and fragility functions derived with structured expert judgment. Journal of Hydrology 603, 126982.

Rahayu, R., S.A. Mathias, S. Reaney, G. Vesuviano, R. Suwarman, and A.M. Ramdhan. 2023. Impact of land cover, rainfall and topography on flood risk in West Java. Natural Hazards 116(2), 1735-1758.

Rahim, M.A., A. Al Assi, R.B. Mostafiz, and C.J. Friedland. 2024. Effects of damage initiation points of depth-damage function on flood risk assessment. Natural Hazards 1(1), 6.

Riedel, L., T. Röösli, T. Vogt, and D.N. Bresch. 2024. Fluvial flood inundation and socio-economic impact model based on open data. Geoscientific Model Development 17(13), 5291-5308.

Ruidas, D., S.C. Pal, A. Saha, P. Roy, C.B. Pande, A.R. Md. T. Islam, and A. Islam. 2024. Flood hazard forecasting and management systems: A review of state-of-the-art modelling, management strategies and policy-practice gap. International Journal of Disaster Risk Reduction 108, 104539.

Storrøsten, E.B., L. Piciullo, F. Nadim, and U. Eidsvig. 2024. Uncertainty in flood risk assessment of linear structures: Why correlation matters. Journal of Hydrology 628, 130442.

Sun, Q., J. Fang, X. Dang, K. Xu, Y. Fang, X. Li, and M. Liu. 2022. Multi-scenario urban flood risk assessment by integrating future land use change models and hydrodynamic models. Natural Hazards and Earth System Sciences 22(11), 3815-3829.

Thao, N.T.P., T.T. Linh, N.T.T. Ha, P.Q. Vinh, and N.T. Linh. 2020. Mapping flood inundation areas over the lower part of the Con River basin using Sentinel 1A imagery. Vietnam Journal of Earth Sciences 42(3), 288-297.

Tu, J., J. Wen, L.E. Yang, A. Reimuth, S.S. Young, M. Zhang, L. Wang, and M. Garschagen. 2023. Assessment of building damage and risk under extreme flood scenarios in Shanghai. Natural Hazards and Earth System Sciences 23(10), 3247-3260.

Venkatappa, M., N. Sasaki, P. Han, and I. Abe. 2021. Impacts of droughts and floods on croplands and crop production in Southeast Asia: An application of Google Earth Engine. Science of the Total Environment 795, 148829.

Zarekarizi, M., K.J. Roop-Eckart, S. Sharma, and K. Keller. 2021. The FLOod Probability Interpolation Tool (FLOPIT): A simple tool to improve spatial flood probability quantification and communication. Water 13(5), 666.

Zhang, H., W. Fang, H. Zhang, and L. Yu. 2021. Assessment of direct economic losses of flood disasters based on spatial valuation of land use and quantification of vulnerabilities: A case study on the 2014 flood in Lishui city of China. Natural Hazards and Earth System Sciences 21(10), 3161-3174.